Propagation of prions causing synucleinopathies in cultured cells

Amanda L. Woerman[a], Jan Stöhr[a,b], Atsushi Aoyagi[a,c], Ryan Rampersaud[a], Zuzana Krejciova[a], Joel C. Watts[a,b,1], Takao Ohyama[c], Smita Patel[a], Kartika Widjaja[a], Abby Oehler[d], David W. Sanders[e], Marc I. Diamond[e], William W. Seeley[b,d], Lefkos T. Middleton[f], Steve M. Gentleman[g], Daniel A. Mordes[h], Thomas C. Südhof[i], Kurt Giles[a,b], and Stanley B. Prusiner[a,b,j,2]

[a]Institute for Neurodegenerative Diseases, University of California, San Francisco, CA 94143; [b]Department of Neurology, University of California, San Francisco, CA 94143; [c]Daiichi Sankyo Company, Limited, Tokyo 140-8710, Japan; [d]Department of Pathology, University of California, San Francisco, CA 94143; [e]Center for Alzheimer's and Neurodegenerative Diseases, University of Texas Southwestern Medical Center, Dallas, TX 75390; [f]Ageing Research Unit, School of Public Health, Imperial College London, London SW7 2AZ, United Kingdom; [g]Centre for Neuroinflammation and Neurodegeneration, Department of Medicine, Imperial College London, London SW7 2AZ, United Kingdom; [h]C. S. Kubik Laboratory for Neuropathology, Department of Pathology, Massachusetts General Hospital, Boston, MA 02114; [i]Department of Molecular and Cellular Physiology and Howard Hughes Medical Institute, Stanford University School of Medicine, Stanford, CA 94305; and [j]Department of Biochemistry and Biophysics, University of California, San Francisco, CA 94143

Contributed by Stanley B. Prusiner, July 8, 2015 (sent for review April 15, 2015)

Increasingly, evidence argues that many neurodegenerative diseases, including progressive supranuclear palsy (PSP), are caused by prions, which are alternatively folded proteins undergoing self-propagation. In earlier studies, PSP prions were detected by infecting human embryonic kidney (HEK) cells expressing a tau fragment [TauRD(LM)] fused to yellow fluorescent protein (YFP). Here, we report on an improved bioassay using selective precipitation of tau prions from human PSP brain homogenates before infection of the HEK cells. Tau prions were measured by counting the number of cells with TauRD(LM)–YFP aggregates using confocal fluorescence microscopy. In parallel studies, we fused α-synuclein to YFP to bioassay α-synuclein prions in the brains of patients who died of multiple system atrophy (MSA). Previously, MSA prion detection required ∼120 d for transmission into transgenic mice, whereas our cultured cell assay needed only 4 d. Variation in MSA prion levels in four different brain regions from three patients provided evidence for three different MSA prion strains. Attempts to demonstrate α-synuclein prions in brain homogenates from Parkinson's disease patients were unsuccessful, identifying an important biological difference between the two synucleinopathies. Partial purification of tau and α-synuclein prions facilitated measuring the levels of these protein pathogens in human brains. Our studies should facilitate investigations of the pathogenesis of both tau and α-synuclein prion disorders as well as help decipher the basic biology of those prions that attack the CNS.

α-synuclein | multiple system atrophy | neurodegeneration | strains | Parkinson's disease

James Parkinson first described a progressive deterioration of the nervous system in 1817 and called it "shaking palsy" (1). Almost one century later, Friederich Heinrich Lewy described the neuropathological hallmark now known as Lewy bodies (LBs) (2). Progress toward discerning the etiology of Parkinson's disease (PD) was achieved 85 years later when the first of several studies identified mutations in or multiplications of the gene encoding α-synuclein, *SNCA*, in inherited cases of PD (3–5). These studies were corroborated by immunostaining for α-synuclein in brain sections from PD patients (6) and subsequently from dementia with Lewy bodies (DLB) cases (7, 8), which found that LBs are surrounded by a halo of α-synuclein polymers.

Along with point mutations in *SNCA* (3), and duplication and triplication of the gene (4, 5) as causes of inherited PD, meta-analysis of genome-wide association studies (9) have identified common variations in *SNCA* as a risk factor for sporadic PD cases. Combined, these data strongly support an etiological role for α-synuclein in the pathogenesis of both the inherited and sporadic forms of PD.

In 1998, brain sections from cases classified as multiple system atrophy (MSA) were analyzed for α-synuclein. Although no LBs were found, abundant immunostaining in the cytoplasm of glial cells was identified (8, 10, 11). A decade earlier, these large immunopositive deposits of α-synuclein were called glial cytoplasmic inclusions (GCIs) based on silver staining (12); they are primarily found in oligodendrocytes but have been occasionally observed in astrocytes and neurons. Limited ultrastructural studies performed on GCIs suggest that they are collections of poorly organized bundles of α-synuclein fibrils (8).

In addition to the accumulation of α-synuclein into LBs in PD and GCIs in MSA, depigmentation of the substantia nigra pars compacta is a hallmark of both PD and the majority of MSA cases (13). This loss of dopaminergic neurons results in diminished input to the basal ganglia that is reflected in the motor deficits exhibited by patients. In the 1990s, fetal tissue transplants into the substantia nigra of PD patients were performed in an attempt to counteract the effects of dopamine loss. Strikingly, upon autopsy of patients that survived at least 10 years posttransplant, LBs were found in the grafted fetal tissue. Because these grafts were no more than 16 years old, the findings argued for host-to-graft transmission of LBs (14, 15). The results of these transplant studies offered evidence supporting the hypothesis that PD is a

Significance

Progressive supranuclear palsy (PSP) and multiple system atrophy (MSA) are neurodegenerative diseases caused by tau and α-synuclein prions, respectively. Prions, purified from human brains of deceased patients with PSP and MSA using phosphotungstic acid, were applied to cultured cell models that selectively form aggregates in the presence of tau or α-synuclein prions, respectively. Whereas brain homogenates prepared from two PSP and six MSA patients infected cultured cells, the same approach was unsuccessful with brain samples from three Parkinson's disease patients. Our findings provide compelling evidence that PSP and MSA are prion diseases, and that MSA is caused by several distinct prion strains.

Author contributions: A.L.W., J.S., K.G., and S.B.P. designed research; A.L.W., J.S., A.A., R.R., Z.K., J.C.W., S.P., K.W., and A.O. performed research; T.O., D.W.S., M.I.D., W.W.S., L.T.M., S.M.G., D.A.M., and T.C.S. contributed new reagents/analytic tools; A.L.W., A.A., R.R., K.G., and S.B.P. analyzed data; and A.L.W., K.G., and S.B.P. wrote the paper.

The authors declare no conflict of interest.

[1]Present address: Tanz Centre for Research in Neurodegenerative Diseases and Department of Biochemistry, University of Toronto, Toronto, ON, Canada M5T 2S8.

[2]To whom correspondence should be addressed. Email: stanley@ind.ucsf.edu.

This article contains supporting information online at www.pnas.org/lookup/suppl/doi:10.1073/pnas.1513426112/-/DCSupplemental.

prion disease, characterized by a misfolded protein that self-propagates and gives rise to progressive neurodegeneration (16, 17). Additional support for this hypothesis came from studies on the spread of α-synuclein deposits from the substantia nigra to other regions of the CNS in PD patients (18).

Even more convincing support for α-synuclein prions came from animal studies demonstrating the transmissibility of an experimental synucleinopathy. The first report used transgenic (Tg) mice expressing human α-synuclein containing the A53T mutation found in familial PD; the mice were designated TgM83 (19). Homozygous mice ($TgM83^{+/+}$) were found to develop spontaneous motor deficits along with increased amounts of insoluble phosphorylated α-synuclein throughout the brain between 8–16 months of age. Ten years later, Mougenot et al. (20) intracerebrally inoculated brain homogenates from sick $TgM83^{+/+}$ mice into ∼2-months-old $TgM83^{+/+}$ mice and found a substantial reduction in the survival time with incubation periods of ∼130 days. Similar observations were reported from two other groups using either homozygous $TgM83^{+/+}$ (21) or hemizygous $TgM83^{+/-}$ (22) mice.

Although our initial attempts to transmit PD to $TgM83^{+/-}$ mice failed (23), the transmission of MSA to the same mouse line was the first demonstration of α-synuclein prions in human brain (22). The $TgM83^{+/-}$ mice, which differ from their homozygous counterparts by not developing spontaneous disease, exhibited progressive CNS dysfunction ∼120 days following intrathalamic inoculation of brain homogenates from two MSA patients. Inoculation of brain fractions enriched for LBs from PD patients into wild-type (WT) mice and macaque monkeys induced aberrant α-synuclein deposits, but neither species developed neurological disease (24). In a similar approach, inoculation of WT mice with the insoluble protein fraction isolated from DLB patients also induced phosphorylated α-synuclein pathology after 15 months, but it failed to induce neurological disease characteristic of DLB (25).

Because α-synuclein prions from MSA patients were transmissible to $TgM83^{+/-}$ mice, we asked whether a more rapid cell-based bioassay could be developed to characterize the MSA prions. With the cell bioassay for progressive supranuclear palsy (PSP) in mind (26, 27), we began by constructing WT and mutant α-synuclein cDNAs fused to yellow fluorescent protein (YFP) (28–30) and expressed these in human embryonic kidney (HEK) cells. By testing the cells with full-length recombinant mutant human α-syn140*A53T fibrils, we induced aggregate formation in HEK cells expressing WT and mutant human *SNCA* transgenes. To expand these findings beyond synthetic prions and to examine natural prions, we report here that phosphotungstic acid (PTA) (31) can be used to selectively precipitate α-synuclein from MSA patients. Screening PTA-precipitated brain homogenate with our cellular bioassay, we detected MSA prions in all six of the cases examined. By measuring the distribution of prions in the substantia nigra, basal ganglia, cerebellum, and temporal gyrus, we found evidence to suggest that at least three different strains of α-synuclein prions may give rise to MSA. We also found that after enrichment by PTA precipitation, ∼6 million α-synuclein molecules comprised an infectious unit of MSA prions in cell culture. Importantly, we transmitted neurodegenerative disease to $TgM83^{+/-}$ mice using PTA-precipitated brain homogenate from an MSA patient, confirming that the aggregate isolation methods used successfully purify prions from patient samples.

Results

In Vitro Detection of Prions. A cell-based approach for detecting prions in human tauopathy samples was recently described (27). Briefly, HEK cells expressing the repeat domain (RD) of tau with two human mutations (P301L and V337M) were created. The mutated tau fragment was fused to YFP using a short linker, resulting in low levels of fluorescence expressed throughout the cytoplasm of the cultured HEK cells. These HEK cells are hereafter referred to as TauRD(LM)–YFP cells. When the cells were incubated with tau prions, the self-propagating, misfolded proteins were able to infect the cells and induce misfolding and aggregation of the TauRD(LM)–YFP fusion protein, similar to the process that occurs in the brains of tauopathy patients. The prion-induced aggregation of mutant tau could be detected by the formation of fluorescent, cytoplasmic aggregates after 12 d. As described here, we adapted this assay to 384-well plates and reduced the time to 4 d to facilitate more rapid analysis of patient samples (Fig. S1).

Detection of Tau Prions in PSP. To identify tau prions from human tauopathy samples, TauRD(LM)–YFP cells were exposed to 1 μg total protein (measured by bicinchoninic acid) from crude brain homogenates (10% wt/vol in PBS), from an aged control brain sample (C2; frontal cortex), or from two PSP brain samples (middle frontal gyrus; Table S1). The two PSP samples gave values of 3.7 ± 0.3% and 4.3 ± 0.4% cells with aggregates, which were indistinguishable from the control sample (C2: 3.6 ± 0.3%; Fig. 1 *A* and *B*). Importantly, this low number of "aggregate-containing" cells in the control sample is an artifact from our aggregate-detection algorithm required to process data in a high-throughput manner; on the low end of aggregate detection, the algorithm is unable to consistently distinguish between real aggregate formation and cells with more fluorescence than others. As a result of this problem, we sought to enhance prion detection in the cell assay above the threshold required for identification of PSP prions. To determine the noise in each plate, we used a brain sample with no evidence of neurodegenerative disease prepared under the same conditions as the diseased brain samples.

In an attempt to increase the number of tau prions infecting the HEK cells, we incubated 10 μg of crude brain homogenate with the cells, but again the PSP samples remained indistinguishable from the control (Table S1). Next, we tried to enhance tau prion detection from PSP patient samples by isolating the prions from the brain homogenates. Initially, we isolated total tau from the samples via immunoprecipitation using the Tau-12 antibody. Whereas tau isolated from the control brain had no effect on the TauRD(LM)–YFP cells (C2: 3.4 ± 0.4%), tau prions isolated from the two PSP cases induced aggregates in 72 ± 16% and 76 ± 7% of the cells (Fig. 1 *A* and *B*; $P < 0.0001$). This result differed from a prior study using two alternative tau antibodies, which showed that immunoprecipitation did not enhance prion detection in TauRD(LM)–YFP cells (27). Because we had previously used sodium PTA to isolate PrP^{Sc} prions (31, 32), we asked whether the same approach might selectively precipitate tau prions from PSP brains. Homogenates (10% wt/vol) prepared from PSP brains were incubated in 2% (vol/vol) sarkosyl and 0.5% (vol/vol) benzonase using an orbital shaker for 2 h. PTA was then added to the solution to a final concentration of 2% (vol/vol), which was then incubated overnight. Next, the sample was centrifuged at 16,000 × *g* for 30 min at room temperature, and the supernatant was removed. The resulting pellet was resuspended in 2% (vol/vol) sarkosyl in PBS and 2% (vol/vol) PTA. The sample was again incubated for at least 1 h before a second centrifugation. The pellet was resuspended in PBS and incubated with the TauRD(LM)–YFP cells in the presence of Lipofectamine 2000, which was found to facilitate rapid and efficient protein uptake into the HEK cells. After 4 d of incubation, the number of cells with YFP aggregates was similar to, albeit slightly lower than, those isolated using immunoprecipitation (PSP1: 65 ± 9.2%; PSP2: 57 ± 5.8%) and significantly increased over the control brain (C2: 2.5 ± 0.2%; Fig. 1 *A* and *B*; $P < 0.0001$).

We confirmed that the TauRD(LM)–YFP cells were responding specifically to tau prions by testing multiple brain regions from 16 additional control samples (C3–C18; Table S2). In addition to the 16 controls, we also tested an MSA patient sample (MSA14); all 17 samples were PTA-precipitated and the resulting pellets were incubated with the TauRD(LM)–YFP cells for 4 d. None of

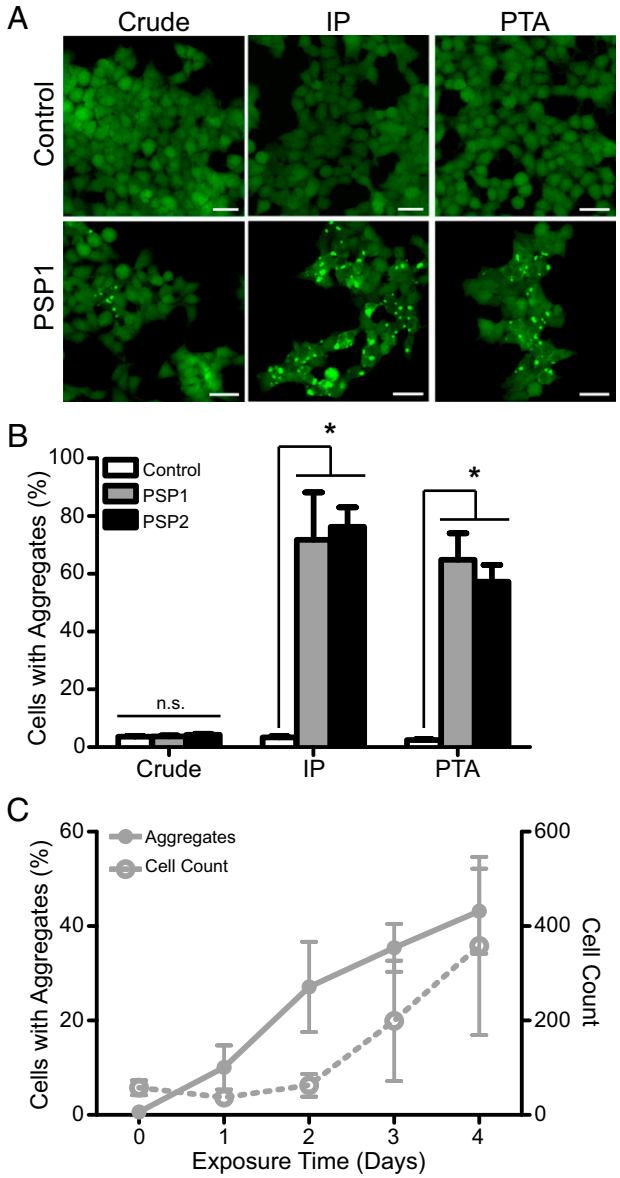

Fig. 1. In vitro detection of tau prions. A rapid, cell-based assay for tau prions is enhanced by precipitating the prion aggregates from human patient samples. (*A*) Representative images of HEK293 cells expressing TauRD(LM)–YFP. Cells were exposed to 1 μg per well of crude brain homogenate (*Left*) from a control patient as well as a PSP patient. (*Right*) Cell infection with PSP following sodium PTA precipitation of prion aggregates; the control sample had no effect. Immunoprecipitation (IP) of tau aggregates using the Tau-12 antibody (*Middle*) was equally effective at isolating tau prions. YFP shown in green. (Scale bars, 100 μm.) (*B*) Quantification of cell infection using a control patient sample along with two PSP patient samples. Precipitating prions from the patient samples before incubating with the cells yielded a significant increase in infectivity. Data shown as mean ± SEM as determined from four images per well in four or six wells; $*P < 0.0001$. (*C*) Quantification of tau aggregate formation in TauRD(LM)–YFP cells every 24 h during incubation with PTA-precipitated prions from patient PSP1. Percentage of cells with aggregates and total cell count shown as mean ± SD. Values measured from the same region of six wells.

the additional controls, including the MSA patient sample, was able to infect the cell line, demonstrating specificity for tau prions.

We characterized PSP prion-induced aggregate formation in the TauRD(LM)–YFP cells using prions that were PTA-precipitated from PSP1 brain homogenate (Fig. 1*C*). We plated 1,000 cells in six wells of a 384-well plate along with tau prions and imaged the plate every 24 h starting immediately after the patient sample was added to the cells (day 0). By analyzing the images through day 4, we found initial aggregate formation in the cells occurred between days 1 and 2, followed by a progressive increase up to day 4. Notably, an exponential increase in the total number of cells occurred between days 1 and 4.

Detection of α-Synuclein Prions in MSA. Mutagenesis studies identifying key α-synuclein mutations for spontaneous aggregate formation (28) and other work testing cell infection using synthetic α-synuclein fibrils (29, 30) led us to ask whether an approach similar to that described above for tau prions might be used to measure α-synuclein prions. We began with 12 cDNA constructs expressing α-synuclein with various mutations and C-terminal truncations fused to YFP that were transfected into HEK cells. From those transfections, we developed 144 clonal cell lines and selected two for testing; one clone expressed full-length WT α-synuclein (α-syn140–YFP) and the second clone expressed full-length α-synuclein harboring the A53T mutation (α-syn140*A53T–YFP). To test these cells, we polymerized full-length synthetic α-syn140*A53T into fibrils, as shown by transmission electron microscopy (Fig. S2*A*), and compared the response of both cell lines to determine the construct yielding the larger dynamic range. In the HEK cells expressing α-syn140–YFP, we found 25–30% of the cells developed aggregates upon exposure to 30 nM α-syn140*A53T fibrils, whereas over 50% of the cells expressing α-syn140*A53T–YFP exhibited aggregates in the presence of the fibrils (Fig. 2). Based on these findings, we chose the α-syn140*A53T–YFP cells for further study.

Knowing that the TauRD(LM)–YFP cells develop aggregates upon exposure to recombinant tau K18 fibrils (27), and that the α-syn140*A53T–YFP cells form aggregates in the presence of α-synuclein fibrils, we tested the specificity of the two cell lines. Using recombinant tau K18 and recombinant α-syn140*A53T fibrils (Fig. S2*A*), we found that the α-syn140*A53T fibrils had no effect on the TauRD(LM)–YFP cells and the tau K18 fibrils had no effect on the α-syn140*A53T–YFP cells (Fig. S2*B*). In addition to recombinant tau K18 and α-syn140*A53T, we also tested Aβ40 fibrils and PBS in both cell lines and found that the cells were unresponsive to both (Fig. S2*C*), highlighting the homotypic specificity of the cells as previously reported (27, 29).

Using brain homogenates prepared from the substantia nigra and surrounding midbrain of three MSA patients (MSA14, MSA15, and

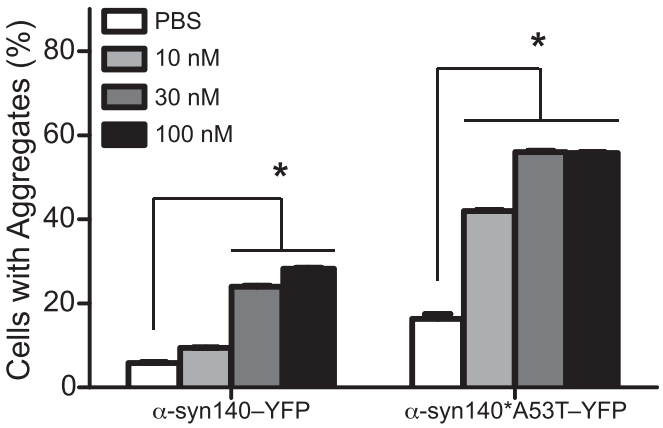

Fig. 2. Response of cell lines to infection with synthetic α-synuclein prions. Two α-synuclein–YFP cell lines were developed and tested for responsiveness to synthetic α-synuclein prions. Quantification of the response of the two α-synuclein–YFP cell lines to increasing concentrations of synthetic α-syn140*A53T fibrils. Data shown as mean ± SEM as determined from four images per well in six wells; $*P < 0.05$.

MSA16), we tested the ability of α-syn140*A53T–YFP cells to form aggregates in the presence of naturally occurring α-synuclein prions. Using crude brain homogenate from the three MSA patients and an aged control patient, we incubated 1 μg of total protein with α-syn140*A53T–YFP cells for 4 d and found the percentage of cells expressing aggregates from each of the three samples was indistinguishable from cells exposed to the control aged brain (Fig. 3 *A* and *B* and Table S3). However, when we PTA-precipitated the samples to isolate aggregated proteins, the cells were able to be infected with α-synuclein prions from the three MSA patient samples but not the control sample (MSA14 and MSA16: $P < 0.0001$; MSA15: $P < 0.05$; Fig. 3 *A* and *B*). These findings were extended by infection with inocula similarly prepared from three additional MSA cases (MSA17–MSA19; Table S3). We then compared the 6 MSA inocula to 16 control samples obtained from deceased people with no known CNS dysfunction following PTA precipitation (Table S2). After incubating the PTA pellets for 4 d, none of these controls or a PSP sample was found to infect the α-syn140*A53T–YFP cells.

To confirm that the infectivity of the MSA patients was due to the presence of WT α-synuclein prions and not a result of templating caused by an A53T mutation in the patient samples, DNA was extracted from all six patient samples and was genotyped by a restriction fragment length polymorphism analysis (3) (Fig. S3). Using Tg mouse DNA originally derived from a patient with a known A53T mutation for comparison, all six MSA patients (MSA14–MSA19) were found to be WT at position 53 of α-synuclein (Fig. S3 and Table S3).

Having shown that PTA precipitation successfully isolates MSA prions from patient samples, and that these prions successfully infect α-syn140*A53T–YFP cells, we characterized the kinetics of aggregate formation in the cells (Fig. 3*C*). Again, we plated 1,000 cells per well in six wells of a 384-well plate and imaged the cells every 24 h following exposure to MSA prions isolated from patient MSA14 (day 0). Aggregate formation increased linearly over 4 d whereas the total cell count increased exponentially between days 2 and 4.

Serial Passage of MSA Prions in Mice. In the MSA transmission experiments that we previously reported, we found MSA patient samples MSA1 and MSA2 induced lethal CNS dysfunction in TgM83$^{+/-}$ mice 143 ± 16 and 106 ± 11 d postinoculation (dpi) (22). To determine whether MSA prions could be propagated in mice, we homogenized the brains of the dead TgM83$^{+/-}$ mice from the primary transmissions and inoculated them into more TgM83$^{+/-}$ mice (Table 1). Not only did we find that we could serially propagate MSA in the mice, but the incubation time for the two inocula decreased (113 ± 13 dpi and 92 ± 5 dpi). We tested the inoculated human MSA brain homogenates used in the original studies, as well as the TgM83$^{+/-}$ mouse brains from the primary and secondary transmissions of the same cases, in the α-syn140*A53T–YFP cells following PTA precipitation. Prions isolated from both MSA cases as well as the primary and secondary transmissions in TgM83$^{+/-}$ mice readily infected the cells, confirming the presence of MSA prions in the mouse brains after passaging. Notably, analysis of DNA isolated from MSA1 and MSA2 found both patients were WT at position 53 in the α-synuclein protein, arguing these results could not be attributed to mutant α-synuclein (Fig. S3).

Synuclein Prions Vary in Brain Distribution Among MSA Patients. Using samples from three MSA patients (MSA14, MSA15, and MSA16), we compared prion levels in the substantia nigra and surrounding midbrain with those in the basal ganglia, cerebellum, and temporal gyrus following PTA precipitation (Fig. 4). The basal ganglia from MSA14 had levels of prions similar to those in the substantia nigra, whereas the cerebellum contained fewer MSA prions and no evidence of prions was found in the temporal gyrus. Interestingly, the substantia nigra from MSA15 was less infectious compared with this brain region in the other two patients (MSA14: 29.3 ± 8.6%; MSA15: 11.2 ± 1.9%; MSA16: 36.2 ± 10.9%; $P < 0.0001$), but the basal ganglia

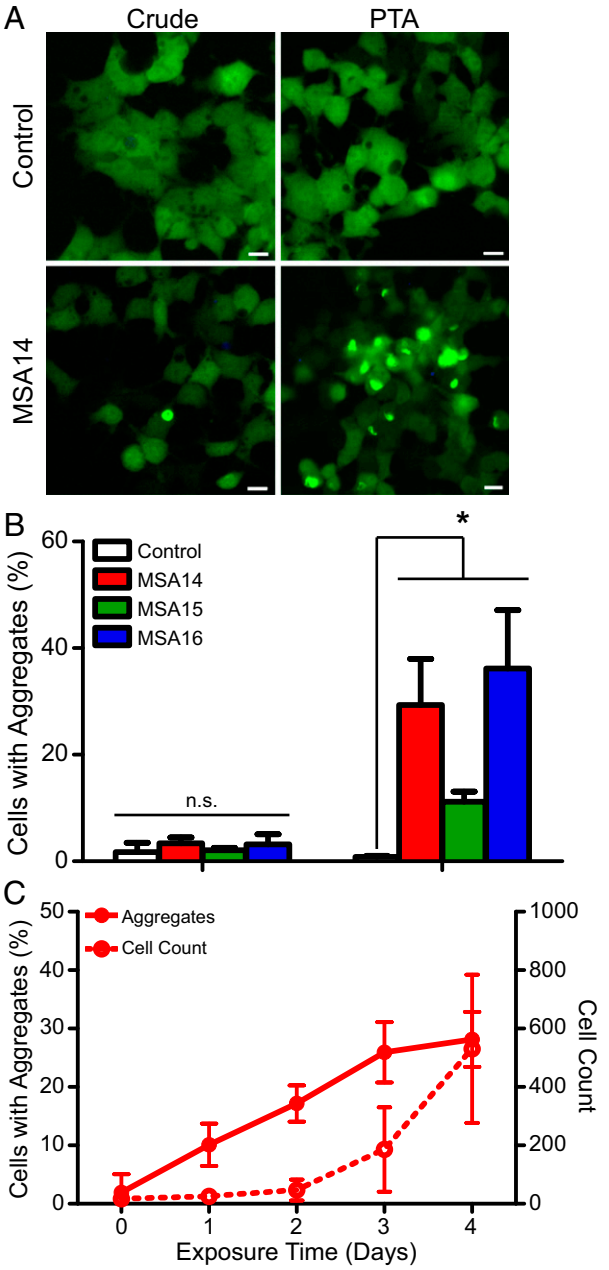

Fig. 3. In vitro detection of α-synuclein prions. A cell-based assay for α-synuclein can detect prions from MSA patient samples. (*A*) Representative images of HEK293T cells expressing α-syn140*A53T–YFP. Cells were exposed to 1 μg per well of crude brain homogenate (*Left*) from a control patient as well as an MSA patient. (*Right*) Cell infection with MSA following sodium PTA precipitation of prion aggregates; the control sample had no effect. YFP shown in green. (Scale bars, 100 μm.) (*B*) Quantification of cell infection using a control patient sample along with three MSA patient samples. Precipitating prions from the patient samples before incubating with the cells yielded a significant increase in infectivity. Data shown as mean ± SD as determined from one image per well from six wells; *$P < 0.05$. (*C*) Quantification of α-synuclein aggregate formation in α-syn140*A53T–YFP cells every 24 h during incubation with PTA-precipitated prions from patient MSA14. Percentage of cells with aggregates (solid line) and total cell count (dashed line) shown as mean ± SD. Values measured from the same region of six wells.

Table 1. In vivo passaging of MSA patient samples and infection of α-syn140*A53T–YFP cells

Inoculum		Primary transmission			Secondary transmission		
Sample	Mean cell infection ± SD,* %	Mean incubation period ± SEM,† dpi	n/n_0	Mean cell infection ± SEM,* %	Mean incubation period ± SEM, dpi	n/n_0	Mean cell infection ± SEM,* %
MSA1	16.2 ± 5.6	143 ± 16	7/8	29.3 ± 3.9, *n = 3*	113 ± 13	6/6	34.1 ± 5.8, *n = 5*
MSA2	45.6 ± 11.1	106 ± 11	8/8	17.9 ± 8.9, *n = 4*	92 ± 5	6/6	47.8 ± 0.7, *n = 2*

*Percentage determinations from six images per well (technical replicates), $n = 6$ wells. Number of mice tested from each experiment (biological replicates) identified as *n*.
†Data reprinted from ref. 22.

(MSA14: 30.3 ± 6.5%; MSA15: 22.5 ± 5.8%; MSA16: 20.1 ± 4.6%; not significant) and cerebellum contained high levels of α-synuclein prion infectivity (MSA14: 15.4 ± 6.2%; MSA15: 23.5 ± 0.9%; MSA16: 7.1 ± 5.2%; $P < 0.001$ for MSA15 vs. MSA16; other comparisons not significant). In both MSA14 and MSA15, prions were undetectable in the temporal gyrus (MSA14: 2.1 ± 0.7%; MSA15: 3.2 ± 1.3%), contrasting with the number of prions detected from the same region of MSA16 (18.9 ± 4.6%; $P < 0.001$). Interestingly, all three patients exhibited a similar pathological distribution of GCIs: frequent GCIs in the cerebellum and white matter of the midbrain (not seen in the substantia nigra) and none in the frontal cortex. The different patterns of MSA prion accumulation in the brain, which did not correspond with the distribution of GCIs, suggest that all three patient samples may contain distinct α-synuclein prion strains, but additional experiments are needed to confirm this finding. Interestingly, these different α-synuclein strains are reminiscent of the different patterns of PrP^{Sc} prion accumulation and lesion profiles found with different strains of scrapie prions (33, 34). Importantly, these differences in α-synuclein prion deposition may contribute to the variations seen in clinical presentations, which often confound the diagnosis of MSA (35, 36).

Characterization of MSA Prions Using the α-syn140*A53T–YFP Assay. To determine the dynamic range of the α-syn140*A53T–YFP cells and the number of α-synuclein molecules required for cell infection in the assay, we isolated MSA prions from the substantia nigra of three patient samples (MSA14, MSA15, and MSA16) using PTA precipitation. The total concentration of α-synuclein in each sample was then quantified via ELISA. Half-log dilutions of the samples were plated with α-syn140*A53T–YFP cells, and the percentage of cells with aggregates was determined for each dilution tested (Fig. 5*A*). Data from the three MSA samples were combined and a nonparametric curve was fit to the data. The same approach was applied to the control sample, and the 95% confidence intervals (CIs) for the two curves were determined (Fig. 5*B*). When the MSA curve became significantly different from the control curve, the point at which the two CIs no longer overlapped, the α-synuclein concentration was 70 pg/mL. This concentration was used to calculate that a minimum of $\sim 6 \times 10^6$ α-synuclein molecules is required for infection of α-syn140*A53T–YFP cells.

In addition, we tested the ability of MSA prions to serially propagate in α-syn140*A53T–YFP cells (Fig. 5*C*). First, PTA-precipitated substantia nigra brain homogenate from MSA14 was used to infect α-syn140*A53T–YFP cells for 4 d before FACS sorting of the cells based upon YFP brightness. Single cells containing aggregates were isolated to develop clonal populations of α-synuclein aggregate-expressing cells. After several passages, we expanded two stable clones (MSA14-2 and MSA14-5) and collected lysate from the cells. We incubated α-syn140*A53T–YFP cells with 0.1, 0.5, 1.0, and 2.0 μg of total protein from the two clones for 4 d and compared the percentage of cells with aggregates to lysate from untransfected HEK cells (Fig. 5*C*). At the lowest concentration tested, neither clone was significantly different from the untransfected lysate (untransfected: 0.7 ± 0.6% cells with aggregates; MSA14-2: 2.7 ± 2.4%; MSA14-5: 2.0 ± 1.4%). When we tested 0.5 μg total protein, both clones infected α-syn140*A53T–YFP cells (MSA14-2: 6.8 ± 4.4%; MSA14-5: 7.0 ± 5.2%) compared with untransfected lysate (0.9 ± 0.9%; $P < 0.05$). Similar results were observed with concentrations of total protein of 1 μg (untransfected: 1.1 ± 0.6%; MSA14-2: 12 ± 3.9%; MSA14-5: 15 ± 4.9%; $P < 0.0001$) and 2 μg (untransfected: 1.3 ± 0.6%; MSA14-2: 10 ± 4.9%; $P < 0.001$; MSA14-5: 8.3 ± 3.1%; $P < 0.01$). Importantly, we tested the MSA14-2 and MSA14-5 lysates in control, untransfected HEK cells to confirm that YFP in the cells was not the result of the YFP-tagged aggregates in the passaged lysate. Lysate from neither clone had any effect on the cells at all four concentrations tested (Fig. 5*C*), indicating that the expression of YFP aggregates represents de novo prion formation in the α-syn140*A53T–YFP cells.

PTA Precipitation Isolates MSA Prions. Having shown that PTA precipitation isolates aggregates from MSA patient samples that are capable of infecting α-syn140*A53T–YFP cells, we asked whether the cells were responding to the same prions that induced neurological dysfunction in the $TgM83^{+/-}$ mice (Fig. 6). To approach this question, we compared a 1% (wt/vol) crude brain homogenate and PTA-precipitated homogenate from patient MSA14. $TgM83^{+/-}$ mice inoculated with crude brain homogenate developed CNS dysfunction with an onset of 130 ± 12 dpi, whereas mice inoculated with the PTA-precipitated sample developed CNS dysfunction at 99 ± 9 dpi (Fig. 6*A*). Pathological analysis of the mouse brains collected from each group based upon immunohistochemistry with the EP1536Y antibody (pSer129) showed phosphorylated α-synuclein aggregates in the brains of the $TgM83^{+/-}$ mice (Fig. 6 *B* and *C*). Notably, the PTA-precipitated sample was 30 times more concentrated than the crude brain homogenate and required ~30 fewer days to cause CNS dysfunction.

Search for α-Synuclein Prions in PD. Having developed a method of isolating MSA prions, we next attempted to isolate α-synuclein prions from the substantia nigra of three PD, three PD with dementia (PDD), and three DLB patient samples using PTA precipitation (Table S3), but none of the nine patient samples was able to infect α-syn140*A53T–YFP cells. To ensure that the lack of infectivity from these samples was not due to less total α-synuclein in these patients, we determined the total α-synuclein concentration in these nine synucleinopathy samples using ELISA after concentrating the aggregates using PTA precipitation (Table S3). It is noteworthy that the MSA, PD, PDD, and DLB patient samples all contained similar amounts of α-synuclein, indicating that the lack of infectivity was not due to low levels of α-synuclein in the samples. We also found all nine patients to be WT at amino acid position 53 in α-synuclein, contending that this difference in infectivity was not due to a difference in primary structure (Table S3 and Fig. S2). Instead, we hypothesize that the lack of demonstrable α-synuclein prion infectivity is due to strain differences (i.e., PD, PDD, and DLB are caused by prions that are distinct from those causing MSA).

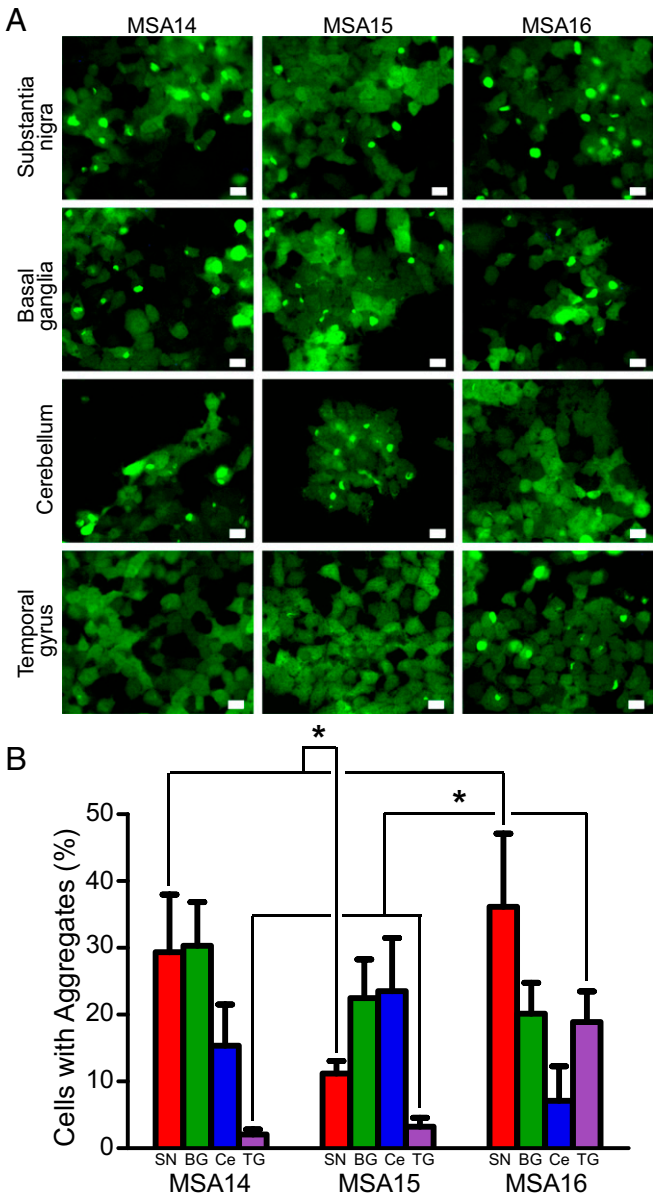

Fig. 4. MSA prion distribution in the brain varies by patient. MSA patients display varied α-synuclein prion distribution throughout multiple brain regions. (*A*) Representative images of α-syn140*A53T–YFP cells infected with sodium PTA-precipitated brain homogenate from the substantia nigra, basal ganglia, cerebellum, and temporal gyrus of three MSA patients. YFP shown in green. (Scale bars, 50 μm.) (*B*) Quantification of cell infections from four brain regions (substantia nigra in red, basal ganglia in green, cerebellum in blue, and temporal gyrus in purple) isolated from three MSA patients shown as mean ± SD. Infectivity of each brain region was compared between all three patients. The substantia nigra from patients MSA14 and MSA16 were significantly more infective than substantia nigra from patient MSA15 ($P < 0.0001$), whereas the temporal gyrus from patient MSA16 was significantly more infective than the temporal gyrus from patients MSA14 and MSA15 ($P < 0.0001$). Values measured from one image taken from each of six wells. BG, basal ganglia; Ce, cerebellum; SN, substantia nigra; and TG, temporal gyrus. *$P < 0.0001$.

Discussion

An expanding body of evidence argues that both Alzheimer's and Parkinson's diseases are caused by prions. Our finding that MSA is transmissible to Tg mice expressing mutant human α-synuclein ($TgM83^{+/-}$) created the first non-PrP prion model of a human disease, with mice developing neurological dysfunction that was accompanied by the accumulation of α-synuclein in multiple brain regions (22). As reported here, MSA prions were serially transmitted with incubation periods slightly decreasing upon a second passage (Table 1). Additionally, we developed a cell culture assay for MSA prions based on our studies with PSP prions as well as earlier work with tau prions (27).

When we adapted a cell-based tau prion bioassay (27) to an automated confocal fluorescence microscopy system, we found the PSP prion infectivity to be too low for reliable measurement. To increase the number of HEK cells with aggregates of TauRD(LM)–YFP, we tried selective precipitation of tau prions from PSP by both immunoprecipitation and PTA precipitation. Both methods were found to substantially increase the number of HEK cells with aggregates of TauRD(LM)–YFP (Fig. 1); between 60–80% of the cells exhibited aggregates after 4 d.

The bioassays for tau and synuclein prions described here using cultured cells are much faster than those previously described for PrP^{Sc} prions using cultured cells (37–39). In contrast to the neuroblastoma cell assays for PrP^{Sc} prions, which require multiple passages to distinguish PrP^{Sc} in the inoculum from that propagating in the cells (40), the bioassays described here were able to measure the levels of PSP or MSA prions within 4 d. Whereas attempts to create PrP fused to green fluorescent protein that could be transformed into a prion were unsuccessful (41, 42), studies with tau and α-synuclein fused to YFP proved to be much more amenable to such modification (27, 43).

As reported here and elsewhere, there was an excellent correlation between the bioassays for α-synuclein prions in $M83^{+/-}$ mice with those in α-syn140*A53T cells (23). MSA prions were detected in α-syn140*A53T cells whether they were selectively precipitated from human brain or after one or two passages in the brains of $M83^{+/-}$ mice. Because earlier studies showed that human PrP^{Sc} prions from the brains of patients with Creutzfeldt–Jakob disease remain infectious after PTA precipitation (44), we investigated precipitating MSA prions with PTA (Fig. 6).

In control experiments, we used recombinant α-syn140*A53T fibrils to compare two different cell lines expressing α-synuclein fusion proteins (Fig. 2). We found that 30 nM fibrils were maximally effective at inducing aggregates in the α-syn140*A53T–YFP cells, whereas others injected fibrils formed from full-length WT human α-syn140 or a 120-residue C-terminally truncated α-synuclein into $TgM83^{+/+}$ mice (21). In addition, WT mice accumulated α-synuclein deposits after a single intrastriatal inoculation of α-synuclein fibrils (45). In these studies, the pathological changes were described as similar to the Lewy pathology of PD; these changes presumably led to a progressive loss of dopaminergic neurons in the substantia nigra, but not in the adjacent ventral tegmental area. The reduced dopamine levels were accompanied by concomitant motor deficits.

Although we could demonstrate α-synuclein prions in PTA-precipitated MSA brain homogenates using α-syn140*A53T–YFP cells, the same protocol failed to detect PD prions. PTA precipitation of putative α-synuclein prions from homogenates prepared from substantia nigra harvested from the brains of three deceased PD patients yielded aggregates that were unable to infect α-syn140*A53T–YFP cells. One explanation for this finding is that PD is caused by α-synuclein prions that represent a strain distinct from that causing MSA. Presumably, these distinct prion strains reflect differences in the tertiary and/or quaternary structures of α-synuclein. Studies by others also suggest the existence of an array of α-synuclein prion strains (46–48). Presumably, α-synuclein prion strains represent different conformers, but currently we must entertain the possibility that a posttranslational chemical modification distinguishes one strain from another. Notably, ubiquitination, phosphorylation, nitrosylation, and sumoylation have all been reported to be covalently bound to α-synuclein (49–52).

Approximately 10% of PD patients carry an inherited mutation resulting in disease. Interestingly, only a small fraction of

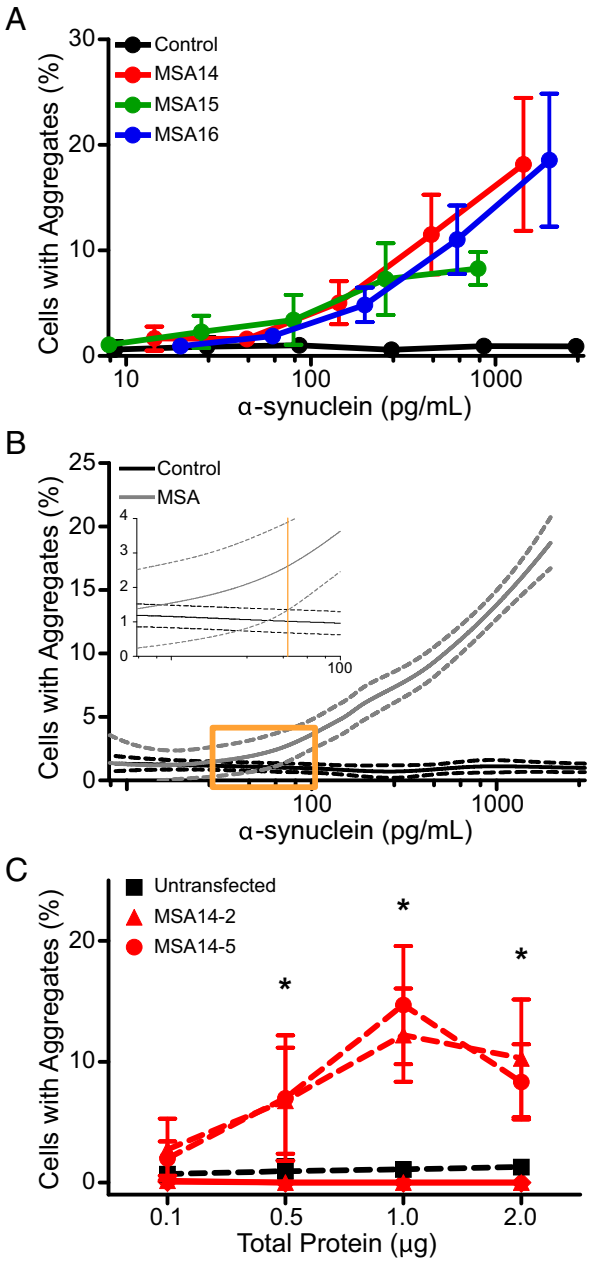

Fig. 5. Characterization of MSA prions by serial dilution and passaging in vitro. The α-syn140*A53T–YFP cells were used to characterize MSA prions in vitro. (*A*) Infectivity curves were generated for four samples (three MSA patient samples and one control patient sample) by plotting the percentage of cells containing aggregates as a function of the total α-synuclein concentration following sodium PTA precipitation, which was determined using half-log dilutions. The curves for all three MSA samples were consistent and distinct from the control sample. Data shown as mean ± SD from one image collected from each of six wells. (*B*) Combining all of the data points for the MSA samples (gray), a nonparametric curve was fit to the data (solid line) and the 95% CI was determined (dashed lines). We determined that the MSA samples became significantly different from the control (black) when the two CIs no longer overlapped at 70 pg/mL (orange line, *Inset*). (*C*) Quantification of infectivity of two α-syn140*A53T–YFP clonal cell lines that stably expressed MSA-induced aggregates (MSA14-2, red triangles, and MSA14-5, red circles) compared with lysate from untransfected HEK293T cells (black squares). Both lysates were tested in the α-syn140*A53T–YFP cell line (dashed red lines) and a nontransgenic HEK293T cell line (solid red lines). Data shown as mean ± SD from one image collected from each of six wells; $*P < 0.05$.

these mutations is found in *SNCA*. The three well-known *SNCA* point mutations are A53T, A30P, and E46K (53), with A53T the most frequently detected (3). Recently, two *SNCA* mutations have been identified in MSA patients presenting with atypical parkinsonism: A53E (54) and G51D (55, 56). More than 22 genes besides *SNCA* have been implicated in causing PD-like movement disorders, that is, parkinsonism (57). Whether any of these genes besides mutant *SNCA* give rise to pathogenic proteins in synucleinopathy patients remains to be established.

An expanding body of evidence argues that both tau and α-synuclein meet all of the requirements necessary to be classified as prions, including the ability to adopt alternative conformations that become self-propagating (58, 59). In the case of tau prions, these replicating protein conformers cause primary tauopathies typified by PSP. Additionally, the accumulation of tau prions in Alzheimer's disease (AD) is thought to be responsible for the dementia that is the most prominent feature of this illness (60). Although Aβ prions are the cause of AD, increasing data argue that Aβ prions induce tau prion formation (61–63). Importantly, evidence for different strains of Aβ prions has been obtained showing that distinct strains cause different patterns of Aβ amyloid deposition (64, 65).

The studies presented here demonstrate that α-synuclein prions are transmissible to cultured HEK cells expressing mutant full-length α-syn140*A53T–YFP. Using these cells, we were able to measure α-synuclein prions in brain extracts prepared from patients who died of MSA. Unexpectedly, similar preparations using brain homogenates from PD patients were unable to initiate the replication of α-synuclein prions. Our findings suggest that the α-synuclein prions causing MSA are distinct from those responsible for PD.

Materials and Methods

All animal procedures were approved by the University of California San Francisco Institutional Animal Care and Use Committee, and all procedures are in accordance with the recommendations of the Panel on Euthanasia of the American Veterinary Medical Association and the National Institutes of Health publication *Guide for the Care and Use of Laboratory Animals* (66).

Human Tissue Samples. Frozen brain tissue samples from two neuropathologically confirmed cases of PSP were received from the University of California, San Francisco (UCSF) Neurodegenerative Disease Brain Bank. Both samples were obtained from the middle frontal gyrus. Frozen brain tissue samples from six neuropathologically confirmed cases of MSA were supplied by the neuropathology core of the Massachusetts Alzheimer's Disease Research Center. The Parkinson's UK Tissue Bank at Imperial College supplied samples from three confirmed PD, three confirmed PDD, and three confirmed DLB patients, and five control samples. All synucleinopathy tissue samples were obtained from the substantia nigra unless otherwise noted. Additional control samples were provided by Martin Ingelsson, Uppsala University, Uppsala, Sweden, and Deborah Mash, University of Miami, Coral Gables, Florida. Patient sex and age at death from all disease samples used in these studies can be found in Table S4.

Patient Neuropathology. The PSP patient samples were received from patients enrolled in UCSF Memory and Aging Center longitudinal clinical research programs. The fresh brains were cut into ~1-cm coronal sections and were alternately fixed in 10% (wt/vol) neutral buffered formalin for 72 h or rapidly frozen. Neuropathological diagnoses were made in accordance with consensus diagnostic criteria (67) using histological and immunohistochemical methods previously described (68). Patient samples were selected by W.W.S.

MSA patient samples were obtained from the Massachusetts Alzheimer Disease Research Center Brain Bank. Fresh brains were bisected longitudinally; one half was coronally sectioned and rapidly frozen, and the other half was fixed in 10% (wt/vol) neutral buffered formalin and then sectioned. Histological evaluation was performed on a set of blocked regions representative for a variety of neurodegenerative diseases; all blocks were stained with Luxol fast blue (LFB) and H&E. On selected blocks, immunohistochemical analysis, including α-synuclein, β-amyloid, and phosphorylated tau, was performed. The neuropathological diagnosis of MSA required the presence of GCIs (69).

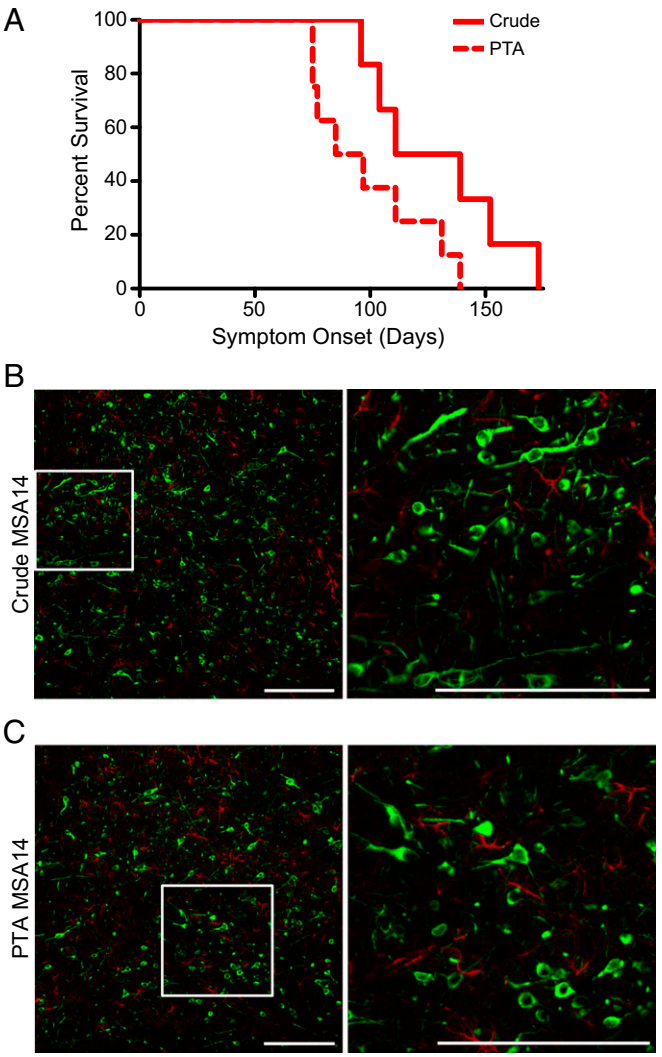

Fig. 6. Sodium PTA precipitates prion aggregates from human patient samples. PTA-precipitated MSA14 brain homogenate induced neurological disease in TgM83$^{+/-}$ following intrathalamic inoculation. (*A*) Kaplan–Meier plot showing the onset of symptoms in two groups of TgM83$^{+/-}$ mice. Mice inoculated with 1% (wt/vol) crude brain homogenate from patient MSA14 (solid red line) developed symptoms with an onset of 130 ± 12 dpi (mean ± SEM). Mice inoculated with PTA-precipitated brain homogenate from MSA14 (dotted red line) developed symptoms in 99 ± 9 dpi. (*B* and *C*) Neuropathology from the reticular formation of TgM83$^{+/-}$ mice inoculated with crude brain homogenate (*B*) or PTA-precipitated brain homogenate (*C*) from patient MSA14 both contain phosphorylated α-synuclein aggregates (EP1536Y, shown in green). Glial fibrillary acidic protein (GFAP) in red. (Scale bars, 200 μm.)

PD, PDD, and DLB patient samples were obtained from the Parkinson's UK Tissue Bank at Imperial College, London. Fresh brains were bisected, with one hemisphere fixed in 10% (wt/vol) buffered formalin for diagnostic workup and the other coronally sliced, photographed on a grid, and then rapidly frozen. Blocks of tissue from 20 key anatomical areas were sampled from the fixed hemisphere. Sections from each area were stained with H&E and LFB. For assessment and staging of neurodegenerative pathology, appropriate sections were stained with antibodies against α-synuclein, β-amyloid, tau, and p62. LB disease cases were staged according to Braak criteria (70), as was the tau pathology (71).

Cell Line Development. HEK293 cells expressing TauRD(LM)–YFP were previously reported (27). The constructs encoding full-length WT and A53T-mutated human α-synuclein fused with YFP at the C terminus were synthesized (GeneArt; Thermo Fisher) and introduced into the pcDNA3.1(+) expression vector (Thermo Fisher). The α-synuclein–YFP constructs were subcloned into the pIRESpuro3 vector (Clontech) using *Eco*RI (5′) and *Not*I (3′).

HEK293T cells (American Type Culture Collection) were cultured in DMEM supplemented with 10% (vol/vol) FBS, 50 units/mL penicillin, and 50 μg/mL streptomycin. Cultures were maintained in a humidified atmosphere of 5% CO_2 at 37 °C. Cells plated in DMEM were transfected using Lipofectamine 2000 (Thermo Fisher). Stable cells were selected in DMEM containing 1 μg/mL puromycin (Thermo Fisher). Monoclonal lines were generated by limiting dilution of polyclonal cell populations in 96- or 384-well plates.

Monoclonal subclones stably expressing α-synuclein aggregates were generated by sorting α-syn140*A53T–YFP cells exposed to MSA patient sample using a Becton Dickinson FACS Aria II. Cells were first gated for a singlet population, followed by a second gate for medium to high YFP expression. A droplet containing a single cell was then plated in each well of a 384-well plate (Greiner); the presence of a clonal population was confirmed using the IN Cell 6000 (GE Healthcare).

Cell Aggregation Assay. Cells were plated in a 384-well plate with black polystyrene walls (Greiner) at a density of 1,000 cells per well with 0.012 μg Hoechst 33342 (Thermo Fisher). Cells were incubated at 37 °C for 2–4 h to allow the cells to adhere to the plate. Lipofectamine 2000 (3% final volume; Thermo Fisher) was added to each patient sample, and the mixture was incubated at room temperature for 1.5 h. OptiMEM (Thermo Fisher) was added to each sample before plating the patient sample in six replicate wells. Plates were then incubated at 37 °C in a humidified atmosphere of 5% CO_2 for 4 d before imaging on the IN Cell 6000. Images of both the DAPI and FITC channels were collected from four different regions in each well. The images were analyzed using the IN Cell Developer software using an algorithm developed to identify intracellular aggregates only in live cells. On the low end of aggregate detection, the algorithm grapples with distinguishing aggregates with cells expressing more fluorescence than the neighboring cells.

Cell Assay Sample Preparation. Immunoprecipitation of PSP patient samples was performed using the Tau-12 monoclonal antibody (72). Culturing and purification methods are described in *Supporting Information*. Tau-12 was biotinylated using the EZ-Link Sulfo-NHS-Biotin kit (Pierce), and 10 μg of antibody was incubated with 100 μL of 10% (wt/vol) crude brain homogenate overnight at 4 °C. The homogenate/antibody mixture was incubated with 100 μL Dynabeads (Thermo Fisher) for 3 h while shaking at 1,000 rpm at 25 °C. After washing in PBS, antibody-bound tau was eluted using 100 mM glycine, pH 2.5, and neutralized with Tris·HCl, pH 8.0. The product was not diluted before incubation with Lipofectamine 2000.

PTA precipitation was performed as described (31, 32). Briefly, 10% (wt/vol) brain homogenate was incubated in 2% (vol/vol) sarkosyl and 0.5% (vol/vol) benzonase (Sigma) at 37 °C with constant agitation (1,200 rpm) in an orbital shaker for 2 h. Sodium PTA was dissolved in double-distilled H_2O, and the pH was adjusted to 7.0. PTA was added to the solution to a final concentration of 2% (vol/vol), which was then incubated overnight in the same conditions. The sample was centrifuged at 16,000 × *g* for 30 min at room temperature, and the supernatant was removed. The resulting pellet was resuspended in 2% (vol/vol) sarkosyl in PBS and 2% (vol/vol) PTA in double-distilled H_2O, pH 7.0. The sample was again incubated for at least 1 h before a second centrifugation. The supernatant was again removed, and the pellet was resuspended in PBS using 10% of the initial starting volume. This suspension was diluted 1:4 in PBS before incubating with Lipofectamine 2000.

Statistical Analysis. PSP, synthetic α-syn140*A53T fibril, and animal inoculation data are presented as mean ± SEM. Cell data represent averages of four images collected from each well of a 384-well plate. Replicates of those images were averaged from six wells, unless otherwise noted. MSA, PD, PDD, DLB, and time course data are presented as mean ± SD. Data represent the averages from one image collected from each of six replicate wells per sample. PSP and MSA data were analyzed for statistical significance using a repeated-measures two-way ANOVA with a Bonferroni post hoc test when crude, IP, and PTA-precipitated samples were compared (data presented in Figs. 1 and 3). All other PSP and MSA data were analyzed using a one-way ANOVA with a Newman–Keuls multiple comparison post hoc test. PD, PDD, and DLB data were analyzed using a Student's *t* test. An F-test was used to determine equal or unequal variance compared with the control sample. Statistical significance for all tests was determined with a *P* value <0.05.

ACKNOWLEDGMENTS. This work was supported by grants from the National Institutes of Health (NIH) (AG002132, AG010770, AG021601, and AG031220) as well as the Rainwater Charitable Foundation, the Sherman Fairchild Foundation, the Dana Foundation, and the Mary Jane Brinton Fund. PSP

tissue samples were received from the University of California, San Francisco Neurodegenerative Disease Brain Bank, which is supported by the NIH (AG023501 and AG19724 to W.W.S.), the Tau Consortium, and the Consortium for Frontotemporal Dementia Research. Additional tissue samples were supplied by the neuropathology core of the Massachusetts Alzheimer's Disease Research Center (AG005134); the Parkinson's UK Tissue Bank at Imperial College London, funded by Parkinson's UK, a charity registered in England and Wales (948776) and in Scotland (SC037554); and the University of Miami Brain Endowment Bank. DNA for WT and A53T mutated human α-synuclein was kindly provided by Dr. Robert Nussbaum. We thank the Hunter's Point animal facility staff for their assistance with animal experiments and Marta Gavidia for mouse genotyping. Additional thanks to Dr. Joel Gever for optimizing the cell assay conditions and to Ana Serban for the production of the K18 fragment of tau and the anti-Tau-12 antibody.

1. Parkinson J (1817) *An Essay on the Shaking Palsy* (Sherwood, Neely, and Jones, London).
2. Forster E, Lewy FH (1912) Paralysis agitans. *Pathologische Anatomie. Handbuch der Neurologie*, ed Lewandowsky M (Springer, Berlin), pp 920–933.
3. Polymeropoulos MH, et al. (1997) Mutation in the α-synuclein gene identified in families with Parkinson's disease. *Science* 276(5321):2045–2047.
4. Singleton AB, et al. (2003) α-Synuclein locus triplication causes Parkinson's disease. *Science* 302(5646):841.
5. Chartier-Harlin MC, et al. (2004) Alpha-synuclein locus duplication as a cause of familial Parkinson's disease. *Lancet* 364(9440):1167–1169.
6. Spillantini MG, et al. (1997) Alpha-synuclein in Lewy bodies. *Nature* 388(6645): 839–840.
7. Baba M, et al. (1998) Aggregation of alpha-synuclein in Lewy bodies of sporadic Parkinson's disease and dementia with Lewy bodies. *Am J Pathol* 152(4):879–884.
8. Spillantini MG, et al. (1998) Filamentous α-synuclein inclusions link multiple system atrophy with Parkinson's disease and dementia with Lewy bodies. *Neurosci Lett* 251(3):205–208.
9. Nalls MA, et al.; International Parkinson's Disease Genomics Consortium (IPDGC); Parkinson's Study Group (PSG) Parkinson's Research: The Organized GENetics Initiative (PROGENI); 23andMe; GenePD; NeuroGenetics Research Consortium (NGRC); Hussman Institute of Human Genomics (HIHG); Ashkenazi Jewish Dataset Investigator; Cohorts for Health and Aging Research in Genetic Epidemiology (CHARGE); North American Brain Expression Consortium (NABEC); United Kingdom Brain Expression Consortium (UKBEC); Greek Parkinson's Disease Consortium; Alzheimer Genetic Analysis Group (2014) Large-scale meta-analysis of genome-wide association data identifies six new risk loci for Parkinson's disease. *Nat Genet* 46(9):989–993.
10. Wakabayashi K, Yoshimoto M, Tsuji S, Takahashi H (1998) α-synuclein immunoreactivity in glial cytoplasmic inclusions in multiple system atrophy. *Neurosci Lett* 249(2-3): 180–182.
11. Tu PH, et al. (1998) Glial cytoplasmic inclusions in white matter oligodendrocytes of multiple system atrophy brains contain insoluble α-synuclein. *Ann Neurol* 44(3): 415–422.
12. Papp MI, Kahn JE, Lantos PL (1989) Glial cytoplasmic inclusions in the CNS of patients with multiple system atrophy (striatonigral degeneration, olivopontocerebellar atrophy and Shy-Drager syndrome). *J Neurol Sci* 94(1-3):79–100.
13. Fernagut P-O, Ghorayeb I, Diguet E, Tison F (2005) In vivo models of multiple system atrophy. *Mov Disord* 20(Suppl 12):S57–S63.
14. Kordower JH, Chu Y, Hauser RA, Freeman TB, Olanow CW (2008) Lewy body-like pathology in long-term embryonic nigral transplants in Parkinson's disease. *Nat Med* 14(5):504–506.
15. Li JY, et al. (2008) Lewy bodies in grafted neurons in subjects with Parkinson's disease suggest host-to-graft disease propagation. *Nat Med* 14(5):501–503.
16. Olanow CW, Prusiner SB (2009) Is Parkinson's disease a prion disorder? *Proc Natl Acad Sci USA* 106(31):12571–12572.
17. Aguzzi A, Rajendran L (2009) The transcellular spread of cytosolic amyloids, prions, and prionoids. *Neuron* 64(6):783–790.
18. Braak H, et al. (2003) Staging of brain pathology related to sporadic Parkinson's disease. *Neurobiol Aging* 24(2):197–211.
19. Giasson BI, et al. (2002) Neuronal α-synucleinopathy with severe movement disorder in mice expressing A53T human α-synuclein. *Neuron* 34(4):521–533.
20. Mougenot A-L, et al. (2012) Prion-like acceleration of a synucleinopathy in a transgenic mouse model. *Neurobiol Aging* 33(9):2225–2228.
21. Luk KC, et al. (2012) Intracerebral inoculation of pathological α-synuclein initiates a rapidly progressive neurodegenerative α-synucleinopathy in mice. *J Exp Med* 209(5): 975–986.
22. Watts JC, et al. (2013) Transmission of multiple system atrophy prions to transgenic mice. *Proc Natl Acad Sci USA* 110(48):19555–19560.
23. Prusiner SB, et al. Evidence for α-synuclein prions causing multiple system atrophy in humans with parkinsonism. *Proc Natl Acad Sci USA*, 10.1073/pnas.1514475112.
24. Recasens A, et al. (2014) Lewy body extracts from Parkinson disease brains trigger α-synuclein pathology and neurodegeneration in mice and monkeys. *Ann Neurol* 75(3):351–362.
25. Masuda-Suzukake M, et al. (2013) Prion-like spreading of pathological α-synuclein in brain. *Brain* 136(Pt 4):1128–1138.
26. Kfoury N, Holmes BB, Jiang H, Holtzman DM, Diamond MI (2012) Trans-cellular propagation of Tau aggregation by fibrillar species. *J Biol Chem* 287(23):19440–19451.
27. Sanders DW, et al. (2014) Distinct tau prion strains propagate in cells and mice and define different tauopathies. *Neuron* 82(6):1271–1288.
28. Burré J, Sharma M, Südhof TC (2012) Systematic mutagenesis of α-synuclein reveals distinct sequence requirements for physiological and pathological activities. *J Neurosci* 32(43):15227–15242.
29. Holmes BB, et al. (2014) Proteopathic tau seeding predicts tauopathy in vivo. *Proc Natl Acad Sci USA* 111(41):E4376–E4385.
30. Luk KC, et al. (2009) Exogenous alpha-synuclein fibrils seed the formation of Lewy body-like intracellular inclusions in cultured cells. *Proc Natl Acad Sci USA* 106(47): 20051–20056.
31. Safar J, et al. (1998) Eight prion strains have $PrP^{(Sc)}$ molecules with different conformations. *Nat Med* 4(10):1157–1165.
32. Levine DJ, et al. (2015) Mechanism of scrapie prion precipitation with phosphotungstate anions. *ACS Chem Biol* 10(5):1269–1277.
33. Bruce ME, McBride PA, Farquhar CF (1989) Precise targeting of the pathology of the sialoglycoprotein, PrP, and vacuolar degeneration in mouse scrapie. *Neurosci Lett* 102(1):1–6.
34. Hecker R, et al. (1992) Replication of distinct scrapie prion isolates is region specific in brains of transgenic mice and hamsters. *Genes Dev* 6(7):1213–1228.
35. Wenning GK, Braune S (2001) Multiple system atrophy: Pathophysiology and management. *CNS Drugs* 15(11):839–852.
36. Watanabe H, et al. (2002) Progression and prognosis in multiple system atrophy: An analysis of 230 Japanese patients. *Brain* 125(Pt 5):1070–1083.
37. Race RE, Fadness LH, Chesebro B (1987) Characterization of scrapie infection in mouse neuroblastoma cells. *J Gen Virol* 68(Pt 5):1391–1399.
38. Butler DA, et al. (1988) Scrapie-infected murine neuroblastoma cells produce protease-resistant prion proteins. *J Virol* 62(5):1558–1564.
39. Mahal SP, et al. (2007) Prion strain discrimination in cell culture: The cell panel assay. *Proc Natl Acad Sci USA* 104(52):20908–20913.
40. Ghaemmaghami S, et al. (2007) Cell division modulates prion accumulation in cultured cells. *Proc Natl Acad Sci USA* 104(46):17971–17976.
41. Bian J, et al. (2006) GFP-tagged PrP supports compromised prion replication in transgenic mice. *Biochem Biophys Res Commun* 340(3):894–900.
42. Barmada SJ, Harris DA (2005) Visualization of prion infection in transgenic mice expressing green fluorescent protein-tagged prion protein. *J Neurosci* 25(24):5824–5832.
43. Frost B, Jacks RL, Diamond MI (2009) Propagation of tau misfolding from the outside to the inside of a cell. *J Biol Chem* 284(19):12845–12852.
44. Safar JG, et al. (2005) Diagnosis of human prion disease. *Proc Natl Acad Sci USA* 102(9):3501–3506.
45. Luk KC, et al. (2012) Pathological α-synuclein transmission initiates Parkinson-like neurodegeneration in nontransgenic mice. *Science* 338(6109):949–953.
46. Guo JL, et al. (2013) Distinct α-synuclein strains differentially promote tau inclusions in neurons. *Cell* 154(1):103–117.
47. Bousset L, et al. (2013) Structural and functional characterization of two alpha-synuclein strains. *Nat Commun* 4:2575.
48. Peelaerts W, et al. (2015) α-Synuclein strains cause distinct synucleinopathies after local and systemic administration. *Nature* 522(7556):340–344.
49. Giasson BI, et al. (2000) Oxidative damage linked to neurodegeneration by selective alpha-synuclein nitration in synucleinopathy lesions. *Science* 290(5493): 985–989.
50. Shimura H, et al. (2001) Ubiquitination of a new form of α-synuclein by parkin from human brain: Implications for Parkinson's disease. *Science* 293(5528):263–269.
51. Fujiwara H, et al. (2002) alpha-Synuclein is phosphorylated in synucleinopathy lesions. *Nat Cell Biol* 4(2):160–164.
52. Krumova P, et al. (2011) Sumoylation inhibits α-synuclein aggregation and toxicity. *J Cell Biol* 194(1):49–60.
53. Hardy J, Cai H, Cookson MR, Gwinn-Hardy K, Singleton A (2006) Genetics of Parkinson's disease and parkinsonism. *Ann Neurol* 60(4):389–398.
54. Pasanen P, et al. (2014) Novel α-synuclein mutation A53E associated with atypical multiple system atrophy and Parkinson's disease-type pathology. *Neurobiol Aging* 35(9):2180.e1–2180.e5.
55. Kiely AP, et al. (2013) α-Synucleinopathy associated with G51D *SNCA* mutation: A link between Parkinson's disease and multiple system atrophy? *Acta Neuropathol* 125(5): 753–769.
56. Lesage S, et al.; French Parkinson's Disease Genetics Study Group (2013) G51D α-synuclein mutation causes a novel parkinsonian-pyramidal syndrome. *Ann Neurol* 73(4):459–471.
57. Fahn S, Jankovic J, Hallett M (2011) *Principles and Practice of Movement Disorders* (Elsevier Saunders, New York), 2nd Ed.
58. Prusiner SB (2014) *Madness and Memory* (Yale Univ Press, New Haven, CT).
59. Walker LC, Jucker M (2015) Neurodegenerative diseases: Expanding the prion concept. *Annu Rev Neurosci* 38:87–103.
60. Arriagada PV, Growdon JH, Hedley-Whyte ET, Hyman BT (1992) Neurofibrillary tangles but not senile plaques parallel duration and severity of Alzheimer's disease. *Neurology* 42(3 Pt 1):631–639.
61. Cohen RM, et al. (2013) A transgenic Alzheimer rat with plaques, tau pathology, behavioral impairment, oligomeric aβ, and frank neuronal loss. *J Neurosci* 33(15): 6245–6256.
62. Choi SH, et al. (2014) A three-dimensional human neural cell culture model of Alzheimer's disease. *Nature* 515(7526):274–278.

63. Murray ME, et al. (2015) Clinicopathologic and ^{11}C-Pittsburgh compound B implications of Thal amyloid phase across the Alzheimer's disease spectrum. *Brain* 138(Pt 5): 1370–1381.
64. Stöhr J, et al. (2014) Distinct synthetic Aβ prion strains producing different amyloid deposits in bigenic mice. *Proc Natl Acad Sci USA* 111(28):10329–10334.
65. Watts JC, et al. (2014) Serial propagation of distinct strains of Aβ prions from Alzheimer's disease patients. *Proc Natl Acad Sci USA* 111(28):10323–10328.
66. National Research Council (2011) *Guide for the Care and Use of Laboratory Animals* (National Academies Press, Washington, DC), 8th Ed.
67. Mackenzie IR, et al. (2010) Nomenclature and nosology for neuropathologic subtypes of frontotemporal lobar degeneration: An update. *Acta Neuropathol* 119(1):1–4.
68. Kim E-J, et al. (2012) Selective frontoinsular von Economo neuron and fork cell loss in early behavioral variant frontotemporal dementia. *Cereb Cortex* 22(2): 251–259.
69. Gilman S, et al. (2008) Second consensus statement on the diagnosis of multiple system atrophy. *Neurology* 71(9):670–676.
70. Alafuzoff I, et al. (2009) Staging/typing of Lewy body related alpha-synuclein pathology: A study of the BrainNet Europe Consortium. *Acta Neuropathol* 117(6): 635–652.
71. Alafuzoff I, et al. (2008) Staging of neurofibrillary pathology in Alzheimer's disease: A study of the BrainNet Europe Consortium. *Brain Pathol* 18(4):484–496.
72. Ghoshal N, et al. (2002) Tau conformational changes correspond to impairments of episodic memory in mild cognitive impairment and Alzheimer's disease. *Exp Neurol* 177(2):475–493.
73. Barghorn S, Biernat J, Mandelkow E (2005) Purification of recombinant tau protein and preparation of Alzheimer-paired helical filaments in vitro. *Methods Mol Biol* 299: 35–51.
74. Stöhr J, et al. (2012) Purified and synthetic Alzheimer's amyloid beta (Aβ) prions. *Proc Natl Acad Sci USA* 109(27):11025–11030.
75. Chandler RL, Fisher J (1963) Experimental transmission of scrapie to rats. *Lancet* 2(7318):1165.